

Table of Contents

Supplementary

| | |
|---|----------|
| <i>Supplementary Methods</i> | 2 |
| Comparing structural variants (SV) between different tools | 2 |
| Assessing accuracy of SVs between different tools using Nanopore..... | 2 |
| Extracting phased intervals | 2 |
| Assessing accuracy of phased assembly using Illumina insert libraries | 3 |
| <i>Supplementary Tables</i> | 3 |
| Supplementary Table S1. Definitions of observations in the multiple sequence alignment. | 3 |
| Supplementary Table S2. Transition probabilities of Hidden Markov Model (HMM) to call SVs..... | 4 |
| Supplementary Table S3. Matrix with the observation probabilities..... | 5 |
| Supplementary Table S5. SV statistics produced by MsPAC. | 6 |
| Supplementary Table S6. Runtime and CPU resources for different MsPAC steps for the HG002 dataset. | 6 |
| Supplementary Table S7. Call sets used for comparison. | 7 |
| Supplementary Table S8. Accuracy of SVs for different tools using ONT reads..... | 7 |
| <i>Supplementary Figures</i> | 8 |
| Supplementary Figure S1. Histogram of haplotype 1 scores across all reads. | 8 |
| Supplementary Figure S2. Overlap between deletions made using different SV callers and GIAB Tier 1 deletion call set..... | 9 |
| Supplementary Figure S3. Number of unique deletions between call sets. | 10 |

Supplementary Methods

Comparing structural variants (SV) between different tools

SV call sets from six different tools (pbsv, falcon, smrtsv, sniffles, lumpy, and delly) were downloaded from the GIAB GitHub page (<https://github.com/genome-in-a-bottle>). For each call set, the distance between SVs were calculated. SVs with any coordinates within 1Kb of each other were considered as overlapping between call sets. Plotting the size of the SVs that “overlapped” showed a high correlation (data not shown). Supplementary Figure S1 shows the percentage of overlap between deletions in the call sets. For example, 86.4% of the deletions identified by MsPAC were found by pbsv, and 84.0% of the deletions identified by pbsv were found by MsPAC. Supplementary Figure 2 shows the number of unique deletions found in each call set. For example, 874 deletions identified by MsPAC were not found by pbsv, and 981 deletions identified by pbsv were not found by MsPAC.

Assessing accuracy of SVs between different tools using Nanopore

Insertion events called by pbsv, falcon, MsPAC and smrtsv were evaluated by comparing against Oxford Nanopore Technology (ONT) reads derived from the AJ sample (ftp://ftp-trace.ncbi.nlm.nih.gov/giab/ftp/data/AshkenazimTrio/HG002_NA24385_son/Ultralong_OxfordNanopore/combined_2018-05-18/combined_2018-05-18.fastq.gz). In each case, the predicted insertion sequence from each caller was inserted *in silico* into the reference at the predicted location, ONT reads were aligned both to the reference and the created insertion reference, and an alignment score was calculated for each. Alignment scores were calculated as the alignment length minus the number of gaps divided by the alignment length. A predicted insertion was considered false if the majority of ONT reads aligned preferentially to the reference. The same procedure was performed for deletions identified by pbsv, falcon, MsPAC, smrtsv, sniffles, lumpy, and delly. Supplementary Table 6 shows the accuracy score for each tool.

Extracting phased intervals

We obtained phased SNVs from 10X (ftp://ftp-trace.ncbi.nlm.nih.gov/giab/ftp/data/AshkenazimTrio/analysis/10XGenomics_ChromiumGenome_LongRanger2.0_06202016/HG002_NA24385_son/). To extract haplotype intervals we used WhatsHap version 0.18, with the command: `whatshap stats <input_vcf> --block-list <regions.bed>`.

Assessing accuracy of phased assembly using Illumina insert libraries

Two different Illumina datasets, 2x250bp (350bp insert) paired-end reads and 6Kb mate pairs reads, were downloaded from ftp://ftp-trace.ncbi.nlm.nih.gov/giab/ftp/data/AshkenazimTrio/HG002_NA24385_son/NIST_Illumina_2x250bps/ and ftp://ftp-trace.ncbi.nlm.nih.gov/giab/ftp/data/AshkenazimTrio/HG002_NA24385_son/NIST_Stanford_Illumina_6kb_matepair/fastqs. Each pair of the mate pairs and paired-end reads were aligned to the HG002 assembly separately using BWA mem. The number of mates mapping to the same haplotype were first determined. The mapping was then filtered to select alignments with a mapping quality score greater than 30. The number of mates mapping to the same haplotype increased to 99.6% and 98.5% when the filter was applied to the 2x250bp Illumina library and the 6Kb mate pair Illumina library.

Supplementary Tables

| Observation | Explanation | Example | | |
|-------------|---------------------------------------|------------|------------|----------------|
| | | Hap 1 base | Hap 2 base | Reference base |
| 0 | no mutation | A | A | A |
| 1 | heterozygous SNV on haplotype 1 | A | T | T |
| 2 | homozygous SNV | A | A | T |
| 3 | heterozygous SNV on haplotype 2 | A | T | A |
| 4 | heterozygous multi-allele | A | T | C |
| 5 | heterozygous insertion on haplotype 1 | A | - | - |
| 6 | heterozygous deletion on haplotype 1 | - | A | A |
| 7 | heterozygous deletion on haplotype 2 | A | - | A |
| 8 | heterozygous deletion/multi-allele | A | - | T |
| 9 | heterozygous insertion on haplotype 2 | - | A | - |
| 10 | homozygous insertion | A | A | - |
| 11 | homozygous insertion/multi-allele | A | T | - |
| 12 | homozygous deletion | - | - | A |
| 13 | heterozygous deletion/multi-allele | - | A | T |
| 14 | Gap sequence | A | A | N |

Supplementary Table S1. Definitions of observations in the multiple sequence alignment.

Each state models 15 observations. An observation is a column in the multiple sequence alignment between the reference and both haplotypes. The table shows the modelled observations and an example of an observation.

| | | | | Current state | | | | | | | | | | Complex | Normal | | | |
|------------|-----------|---------|-----|---------------|-------|-------|---------|-------|----------|-------|-------|---------|-------|---------|--------|-------|--------------------------|-------|
| | | | | Insertion | | | | | Deletion | | | | | | | | | |
| | | | | Normal | | | Complex | | Normal | | | Complex | | | | | | |
| | | | | 1 1 | 0 1 | 1 0 | 1 1 | 0 1 | 1 0 | 1 1 | 0 1 | 1 0 | 1 1 | | | 0 1 | 1 0 | |
| Next state | Insertion | Normal | 1 1 | .9999 | | | | | | | | | | | | 6e-14 | | |
| | | | 0 1 | | .9999 | | | | | | | | | | | | 6e-14 | |
| | | | 1 0 | | | .9999 | | | | | | | | | | | | 6e-14 |
| | | Complex | 1 1 | | | | .9999 | | | | | | | | | | | 6e-14 |
| | | | 0 1 | | | | | .9999 | | | | | | | | | | 6e-14 |
| | | | 1 0 | | | | | | .9999 | | | | | | | | | 6e-14 |
| | Deletion | Normal | 1 1 | | | | | | .9999 | | | | | | | | 6e-14 | |
| | | | 0 1 | | | | | | | .9999 | | | | | | | 6e-14 | |
| | | | 1 0 | | | | | | | | .9999 | | | | | | 6e-14 | |
| | | Complex | 1 1 | | | | | | | | | .9999 | | | | | 6e-14 | |
| | | | 0 1 | | | | | | | | | | .9999 | | | | 6e-14 | |
| | | | 1 0 | | | | | | | | | | | .9999 | | | 6e-14 | |
| | Complex | | | | | | | | | | | | | | .9999 | 6e-14 | | |
| | Normal | | | .0001 | .0001 | .0001 | .0001 | .0001 | .0001 | .0001 | .0001 | .0001 | .0001 | .0001 | .0001 | .0001 | 0.999999 9999992 2 | |

Supplementary Table S2. Transition probabilities of Hidden Markov Model (HMM) to call SVs. The table shows the transitional probabilities between the 14 states. Every entry in the table that is not filled are states that are not connected in the HMM. Every state except the normal state can transition to itself or to the normal state, as represented in the table. The normal state can transition into any other state. We chose balanced probabilities for entering events so as to not bias the choice of event types. Transition probability to the normal state was set to .0001 to encourage longer SVs.

| Obs. | State | | | | | | | | | | | | Complex | Normal |
|------|------------|------------|------------|------------|------------|------------|------------|------------|------------|------------|------------|------------|-------------|------------|
| | Insertion | | | | | | Deletion | | | | | | | |
| | Normal | | | Complex | | | Normal | | | Complex | | | | |
| | 1 1 | 0 1 | 1 0 | 1 1 | 0 1 | 1 0 | 1 1 | 0 1 | 1 0 | 1 1 | 0 1 | 1 0 | | |
| 0 | .004 | .004 | .004 | <u>.01</u> | <u>.01</u> | <u>.01</u> | .004 | .004 | .004 | <u>.01</u> | <u>.01</u> | <u>.01</u> | .006 | <u>.95</u> |
| 1 | .004 | .004 | .004 | .004 | .004 | .004 | .004 | .004 | .004 | .004 | .004 | .004 | .006 | .004 |
| 2 | .004 | .004 | .004 | .004 | .004 | .004 | .004 | .004 | .004 | .004 | .004 | .004 | .006 | .004 |
| 3 | .004 | .004 | .004 | .004 | .004 | .004 | .004 | .004 | .004 | .004 | .004 | .004 | .006 | .004 |
| 4 | .004 | .004 | .004 | .004 | .004 | .004 | .004 | .004 | .004 | .004 | .004 | .004 | .006 | .004 |
| 5 | .004 | <u>.95</u> | .004 | .004 | <u>.94</u> | .004 | .004 | .004 | .004 | .004 | .004 | .004 | <u>.158</u> | .004 |
| 6 | .004 | .004 | .004 | .004 | .004 | .004 | .004 | .004 | <u>.95</u> | .004 | .004 | <u>.94</u> | <u>.158</u> | .004 |
| 7 | .004 | .004 | .004 | .004 | .004 | .004 | .004 | <u>.95</u> | .004 | .004 | <u>.94</u> | .004 | <u>.158</u> | .004 |
| 8 | .004 | .004 | .004 | .004 | .004 | .004 | .004 | .004 | .004 | .004 | .004 | .004 | .006 | .004 |
| 9 | .004 | .004 | <u>.95</u> | .004 | .004 | <u>.94</u> | .004 | .004 | .004 | .004 | .004 | .004 | <u>.158</u> | .004 |
| 10 | <u>.95</u> | .004 | .004 | <u>.94</u> | .004 | .004 | .004 | .004 | .004 | .004 | .004 | .004 | <u>.158</u> | .004 |
| 11 | .004 | .004 | .004 | .004 | .004 | .004 | .004 | .004 | .004 | .004 | .004 | .004 | .006 | .004 |
| 12 | .004 | .004 | .004 | .004 | .004 | .004 | <u>.95</u> | .004 | .004 | <u>.94</u> | .004 | .004 | <u>.158</u> | .004 |
| 13 | .004 | .004 | .004 | .004 | .004 | .004 | .004 | .004 | .004 | .004 | .004 | .004 | .006 | .004 |
| 14 | .004 | .004 | .004 | .004 | .004 | .004 | .004 | .004 | .004 | .004 | .004 | .004 | .006 | .004 |

Supplementary Table S3. Matrix with the observation probabilities. The emission probability (observation probability) for each observation and for each state is listed in the table. In this study, for non-complex events we set the probability of observing the expected state to 95% (lowering it to 94% for complex variants and allowing for more “normal” bases). For fully “complex” events, we distributed the various insertion/deletion states evenly under the assumption no specific event-type was preferred.

| Haplotype | Coverage (no ambig. reads) | Coverage (ambig. reads included) | Bases assembled | % of chr1-22 assembled | N50 | Longest contig |
|-----------|----------------------------|----------------------------------|-----------------|------------------------|-------|----------------|
| 1 | 26.6 | 52.4 | 2.45GB | 91.4% | 4.3MB | 22.7MB |
| 2 | 26.8 | 52.5 | 2.47GB | 91.8% | 4.2MB | 21.3MB |

Supplementary Table S4. MsPAC haplotype assembly statistics. The table shows the assembly statistics for each haplotype assembled by MsPAC.

| SV | Homozygous | Heterozygous (SV in haplotype 1) | Heterozygous (SV in haplotype 2) | Validation rate using ONT | SVs containing TRs* |
|-------------------|------------|----------------------------------|----------------------------------|---------------------------|---------------------|
| Deletion | 2,375 | 2,021 | 2,014 | 95% (2,947/3,113) | 2,780 |
| Insertion | 4,420 | 2,367 | 2,465 | 87% (3,438/3,930) | 5,431 |
| Complex Deletion | 421 | 729 | 337 | 72% (150/207) | 327 |
| Complex Insertion | 646 | 721 | 288 | 74% (147/198) | 653 |
| Complex | 112 | NA | NA | NA | 54 |

Supplementary Table S5. SV statistics produced by MsPAC. The table shows the number of different SVs identified separated by genotype, with the validation rate using ONT reads.

| MsPAC step | Max runtime per job | Max resources per job | Number of jobs | Total CPU runtime |
|-----------------------------|---------------------|-----------------------|---------------------------|-------------------|
| Phasing | < 4 hours | 2 GBs, 1 core | 22 (or # of chromosomes) | ~ 30 hours |
| Separating raw PacBio reads | < 20 hours | 40GBs, 1 core | 22 (or # of chromosomes) | ~100 hours |
| Assembly | < 30 min | 8 GBs, 1 core | < 10,000 | ~2,260 hours |
| SV detection | < 20 min | 2 GBs. 1 core | ~ 10,000 | ~350 hours |

Supplementary Table S6. Runtime and CPU resources for different MsPAC steps for the HG002 dataset. The table shows the runtime and CPU resources needed for each job for each specific MsPAC step and the number of jobs per step. The whole process takes 3 – 8 days depending on the number of jobs distributed to the cluster and availability of the cluster.

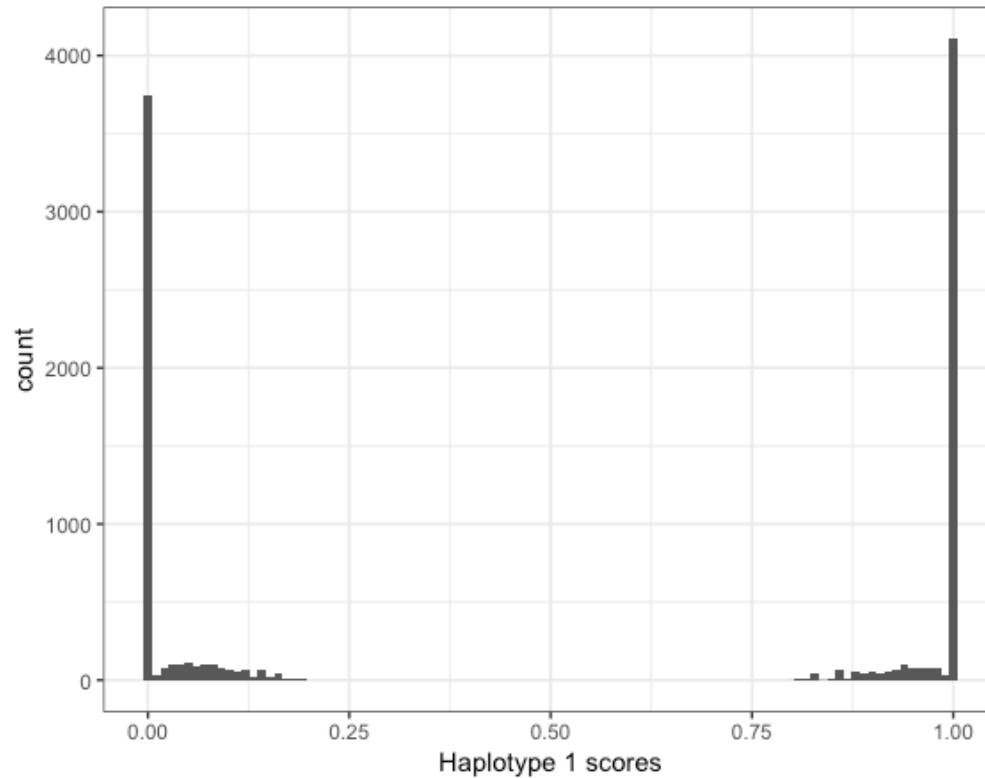
| Call set (version, if found) | URL |
|------------------------------|---|
| PbHoney (svn revision 107) | ftp://ftp-trace.ncbi.nlm.nih.gov/giab/ftp/data/AshkenazimTrio/analysis/BCM_PacBio_PBHoney_Sep.8.2016_Filt/Calls.bed |
| smrtsv (June 2016) | ftp://ftp-trace.ncbi.nlm.nih.gov/giab/ftp/data/AshkenazimTrio/analysis/Chaisson_PacBio_smrt-sv.dip_Jun2016/deletions.bed, ftp://ftp-trace.ncbi.nlm.nih.gov/giab/ftp/data/AshkenazimTrio/analysis/Chaisson_PacBio_smrt-sv.dip_Jun2016/insertions.bed |
| Pbsv (v0.1-prerelease) | ftp://ftp-trace.ncbi.nlm.nih.gov/giab/ftp/data/AshkenazimTrio/analysis/PacBio_pbsv_05052017/hg19.HG002.pbsv.vcf.gz |
| sniffles | ftp://ftp-trace.ncbi.nlm.nih.gov/giab/ftp/data/AshkenazimTrio/analysis/Baylor_sniffles_05092017/all_reads.fa.giab_h002_ngmlr-0.2.3_mapped.bam.sniffles1kb_auto_noalts.vcf.gz |
| delly | ftp://ftp-trace.ncbi.nlm.nih.gov/giab/ftp/data/AshkenazimTrio/analysis/DNAexus_AndrewC_Illumina_Callers_Sep2016/HG002/HG002.140528_D00360_0018_AH8VC6ADXX.realigned.recalibrated.delly.deletion.vcf.gz |
| lumpy | ftp://ftp-trace.ncbi.nlm.nih.gov/giab/ftp/data/AshkenazimTrio/analysis/DNAexus_AndrewC_Illumina_Callers_Sep2016/HG002/HG002.140528_D00360_0018_AH8VC6ADXX.realigned.recalibrated.lumpy.vcf |
| GIAB Tier 1 call set | ftp://ftp-trace.ncbi.nlm.nih.gov/giab/ftp/data/AshkenazimTrio/analysis/NIST_SVs_Integration_v0.6/HG002_SVs_Tier1_v0.6.vcf.gz |
| Falcon | ftp://ftp-trace.ncbi.nlm.nih.gov/giab/ftp/data/AshkenazimTrio/analysis/MtSinai_PacBio_Assembly_falcon_03282016/ |

Supplementary Table S7. Call sets used for comparison. The table shows the URL of different SVs call sets. The Falcon call set was generated by applying the SV-calling pipeline from MsPAC on the Falcon assembled contigs.

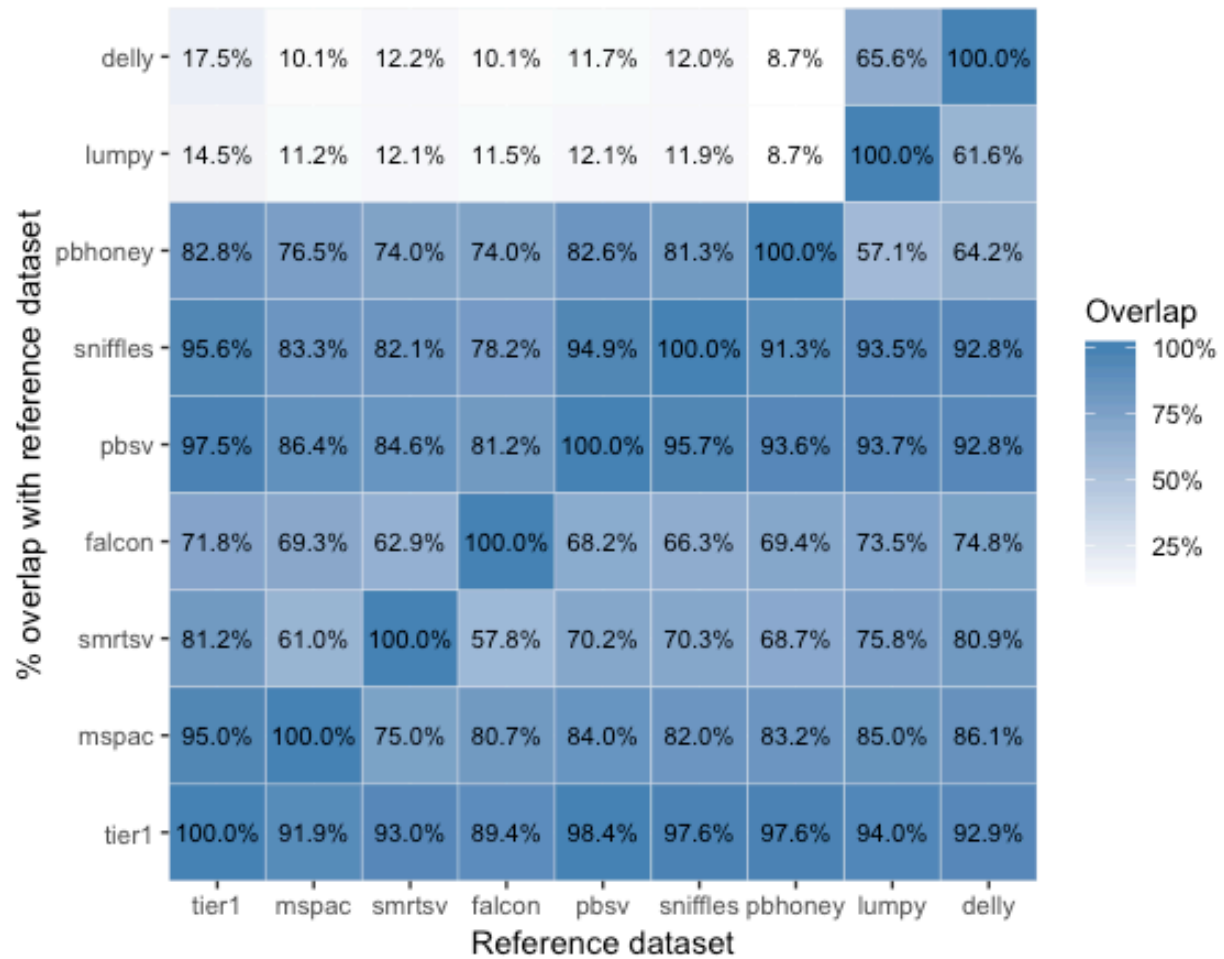
| SV | Tool | Incorrect | Total | Precision |
|-----------|----------|------------|-------------|--------------|
| Deletion | Falcon | 149 | 2474 | 94.0% |
| | MsPAC | 166 | 3113 | 94.7% |
| | smrtsv | 138 | 2850 | 95.2% |
| | Pbhoney | 207 | 2925 | 92.9% |
| | pbsv | 78 | 3345 | 97.6% |
| | sniffles | 76 | 3115 | 97.6% |
| | delly | 8 | 444 | 98.2% |
| | lumpy | 15 | 412 | 96.4% |
| Insertion | Falcon | 442 | 3432 | 87.1% |
| | MsPAC | 492 | 3930 | 87.5% |
| | smrtsv | 405 | 3562 | 88.6% |
| | pbsv | 670 | 4531 | 85.2% |

Supplementary Table S8. Accuracy of SVs for different tools using ONT reads. The table shows the insertion and deletion accuracy for each of the tools tested

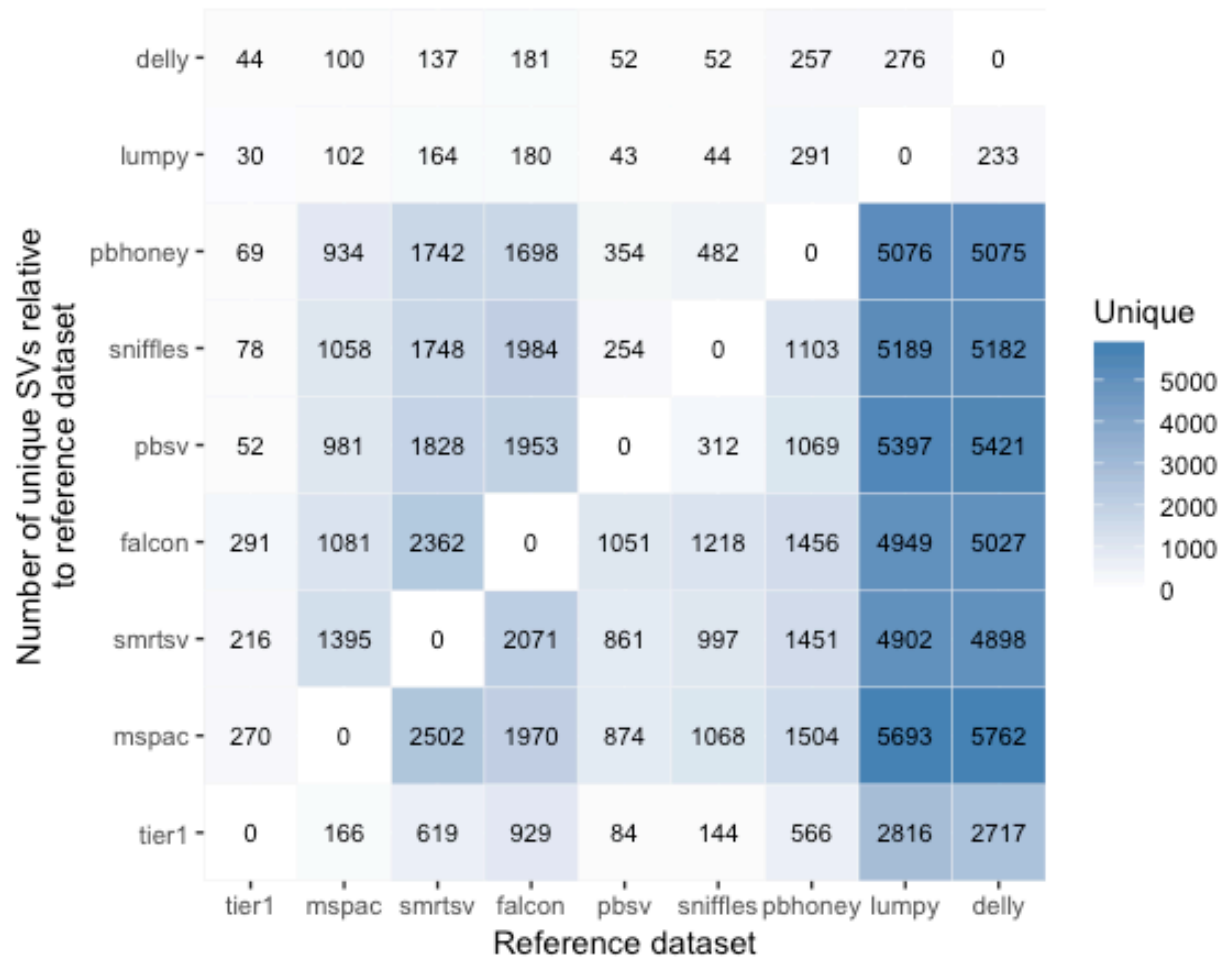
Supplementary Figures



Supplementary Figure S1. Histogram of haplotype 1 scores across all reads. For each read, we plot $\frac{P(r|h_r=1)}{P(r|h_r=1)+P(r|h_r=2)}$, which shows a bimodal distribution. Reads with a score near 1 are likely to be from haplotype 1 and those with a value near 0 are likely to be derived from haplotype 2.



Supplementary Figure S2. Overlap between deletions made using different SV callers and GIAB Tier 1 deletion call set. The matrix shows the overlap of deletions between different tools and GIAB Tier 1 deletions, with each cell showing the percent pairwise overlap.



Supplementary Figure S3. Number of unique deletions between call sets. The matrix shows the unique deletions identified by each tool and GIAB Tier 1 deletion call set on the Y axis when compared the reference dataset in the X axis.